The energy dissipation in turbulent shear flows

K. R. Sreenivasan

Mason Laboratory, Yale University

New Haven, CT 06520-8286

Abstract

From an analysis of grid turbulence data, it was earlier confirmed [1] that the average energy dissipation rate indeed scales on the energy-containing length and velocity scales beyond a microscale Reynolds number of about 100. In this paper, experimental data in various shear flows are examined to determine the effects of mean shear and nearness to boundaries on this scaling. For homogeneous shear flows, it is shown that the shear has a weak but discernible effect— at least at moderate Reynolds numbers—on the scaling of the dissipation rate. For inhomogeneous and unbounded shear flows such as wakes and jets, the scaling of both the local dissipation rate and that integrated across the flow are examined. For the latter, semi-theoretical estimates are provided on the basis of the asymptotic form of development of these flows. The low-Reynolds-number behavior is also examined for wakes. For wall-bounded flows such as the flat-plate boundary layer, the dissipation due to mean shear is shown to be a vanishingly small fraction of the turbulent part. The contributions to the latter from the near-wall region, the logarithmic region and the outer region of the boundary layer are obtained.

1

1 Introduction

1.1 The background

One of the characteristic features of turbulence is that it is dissipative. The rate at which the turbulent energy gets dissipated per unit mass is given [2] by

$$\varepsilon = \frac{\nu}{2} \left[\frac{\partial u_i}{dx_j} + \frac{\partial u_j}{dx_i} \right]^2 , \tag{1}$$

where ν is the kinematic viscosity of the fluid, u_i is the *turbulent* velocity component in the direction i, and repeated indices imply summation over 1, 2 and 3. It is invariably assumed in the phenomenological picture of turbulence that the average value $\langle \varepsilon \rangle$ of the dissipation rate ε remains finite even in the limit of vanishing viscosity [3], [4], [2]. If v and ℓ represent, respectively, the characteristic velocity and length scales of the viscosity-independent features of turbulence, one should expect a scaling of the form

$$\langle \varepsilon \rangle \ell / v^3 = C, \tag{2}$$

C being a constant of the order unity. The turbulent velocity gradients in this picture diverge typically as the inverse-square-root of the viscosity coefficient ν or as the square-root of a characteristic Reynolds number.

In spite of the importance of Eq. (2), it has so far not been possible to deduce it from the partial differential equations governing turbulent motion. Formal bounds [5] differ from empirical observations by a few orders of magnitude (see also [6]), and it appears, at least for the foreseeable future, that the viability of Eq. (2) has to rest on the support it derives experimentally. For grid turbulence, Batchelor [7] had collected data from experiments of

2

the 1940's and concluded that they were in reasonable agreement with expectations. However, the scatter in the data was too large to be convincing: for example, Saffman [8] saw it fit to remark that a weak power-law or logarithmic variation of C could not be ruled out on the basis of those data. Since that time, more data at much higher Reynolds numbers have become available, and these have been analyzed in [1]. In that paper, we had collected all usable experimental data in grid turbulence and shown that the possible variation of C in Batchelor's plot (aside from the scatter itself) was a low-Reynolds-number effect, and that, for microscale Reynolds numbers[1] above 100 or so, C was indeed a constant. This constant was found to be unity when ℓ was chosen as the longitudinal integral scale and v as the root-mean-square velocity of turbulence. This was the principal result of Ref. [1], from where it is reproduced as Fig. 1.

A few qualifications expressed in Ref. [1] are worth recapitulating. Data from grids of somewhat unusual geometry yield slightly different numerical values for C in Eq. (2), and there was even a suggestion from figure 3 of Ref. [1] that its precise value would depend on the configuration of the grid. However, it is not clear that in all experiments one is far enough away from the grid so as to be uninfluenced equally satisfactorily by the direct effects of the grid; it is also not clear that the relevant length scale has always been measured according to a self-consistent procedure. We are therefore inclined to think of these deviations as exceptions to the rule—though clearly important and to be understood at leisure. It would undoubtedly have been desirable for the measurements to have covered a much wider range of Reynolds numbers,

---

[1]This and other technical terms will be defined at appropriate places in the text.

but Fig. 1 seems convincing enough (recall that the microscale Reynolds number is proportional to the square root of the large scale Reynolds number). For now, therefore, it appears prudent to take the result of Fig. 1 as valid in the "ideal" case of grid turbulence (at least in experiments using biplane grids of square mesh), and ask whether features such as different initial conditions, shear, nearness to solid boundaries, and such other details, have measurable effect on this scaling.[2] There would then be a comprehensive understanding of the gross relation between large scales of motion and dissipative scales. This is the purpose of the paper: we examine the scaling of energy dissipation rate in shear flows—both homogeneous (section 2) and inhomogeneous (sections 3 and 4) and, in particular, wall-bounded flows (section 4) whose special feature is that the effects of viscosity are invariably felt near the wall no matter how high the Reynolds numbers. Of particular interest is the relation between the integrated energy dissipation across the flow and the work done at the wall by friction. A few summary remarks are contained in section 5.

1.2 Preliminary remarks

In grid turbulence, since no energy production occurs except at the grid itself, the measurement of the turbulent energy at different downstream distances allows one to estimate the dissipation rate quite accurately. Many authors

---

[2]The scaling supported by Fig. 1, however interesting, is different from the conventional thinking in the Kolmogorov phenomenology that the energy dissipation scales on the length and velocity scales characteristic of *external* stirring. This view would demand, for instance, that $\langle \varepsilon \rangle$ should scale on the power lost due to pressure drop across the grid. Such a suggestion has not been tested directly. One can imagine some interesting phenomenon to manifest when the "drag crisis" occurs for each of the cylinders making up the grid. There is some scope for interesting work here.

have measured the downstream development of all three components of turbulent energy; even when this is not the case, the three components are sufficiently close to each other that the accurate measurement of any one component (usually the longitudinal component) can provide good estimates for the energy dissipation. The main point is that such estimates are quite reliable because they are based on turbulent energy measurements—which, unlike the direct measurements of the energy dissipation itself, can be made quite accurately. Dissipation measurements in shear flows cannot be made similarly simply. One thus estimates dissipation rate by means of local isotropy as well as Taylor's frozen flow hypothesis (which supposes that turbulence advects with the local mean velocity without any distortion); the uncertainties involved are large enough to make it difficult to compare numerical values from one experiment with those from another. Secondly, the nearly isotropic state of grid turbulence simplifies the specification of the length and velocity scales: all the so-called longitudinal integral scales are equal to each other (roughly twice the so-called transverse length scales) and all velocity components are nearly the same. On the other hand, in shear flows—especially wall-bounded flows—the choice of the length and velocity scales is non-trivial. At the least, some consistent choice has to be made and justified. Finally, there is the issue of spatial variation of all quantities in inhomogeneous shear flows.

2 Homogeneous shear flows

The flow next in simplicity to grid turbulence is that with a linear mean velocity distribution (or constant shear) in the direction x_2, say, transverse to the direction x_1 of the mean flow. Good approximations to such flows have been created in several laboratories (see later) and their evolution has been documented in various degrees of detail. Turbulent fluctuations in these flows are essentially homogeneous in the transverse direction, x_2. These "homogeneous shear flows" are considered in this section.

We shall first consider only those experiments in which the energy dissipation was obtained directly, i.e., by measuring all other terms in the turbulent energy balance equation, without resorting to local isotropy and Taylor's hypothesis. Some details of these experiments are listed in Table 1.

With the exception of Tavoularis and Corrsin [11] and Mulhearn and Luxton [14] (see later), all experimenters have been content to measure the longitudinal integral scale, L_{11}, defined by

$$L_{11} = \int\limits_0^\infty dr \frac{R_{11}(r)}{\langle u_1^2 \rangle}, \tag{3}$$

where R_{11} is the "correlation function" $\langle u_1(x_1, x_2, x_3) u_1(x_1 + r_1, x_2, x_3) \rangle$, u_1 is the velocity component in the direction x_1 of the mean flow, and r_1 is the separation distance[3] in the direction x_1. We are therefore forced to use this

---

[3]Most often in practice, one does not measure the equal-time correlation function in the integrand of Eq. (3) but approximates it by $\langle u_1(x_1, x_2, x_3; t) u_1(x_1, x_2, x_3; t + \Delta t) \rangle$, with Δt interpreted as r_1/U_1, U_1 being the mean velocity in the x_1 direction at the fixed point (x_1, x_2, x_3). It is clear that this can be done if Taylor's hypothesis holds but, in general, one does not have control on the errors introduced in this procedure. Further, the integration in Eq. (3) is usually performed only up to the first zero-crossing of the correlation function, $R_{11}(r)$. The rationale for this procedure is described in [15].

length scale as representative. As already remarked, the question of which energy component should be used is not clear either. The precise choice will make a difference at least numerically. We shall use for v the quantity $\langle u_1^2 \rangle^{1/2}$, mainly because the length scale L_{11} corresponds to the velocity component u_1, and because it is this component that has been measured most often. Other choices, such as $(\frac{1}{3}\langle q^2 \rangle)^{\frac{1}{2}}$, where $q^2 = u_i u_i$, have been examined, and do not produce a qualitatively different result.

One additional remark is useful. The Reynolds number most suitable for comparing different experiments is the microscale Reynolds number $R_\lambda \equiv \langle u_1^2 \rangle^{\frac{1}{2}} \lambda / \nu$, based on the Taylor microscale $\lambda = (\frac{<u_1^2>}{<(\partial u_1/\partial x_1)^2>})^{\frac{1}{2}}$. A proper non-dimensional measure of the shear is the parameter $S \equiv \frac{<q^2>}{<\varepsilon>} |\frac{dU_1}{dx_2}|$, whose interpretation can be found, among other places, in [16] (see also the appendix in Ref. [12]): briefly, $\frac{<q^2>}{<\varepsilon>}$ is a representative time scale of turbulence and normalizes the mean rate of strain dU_1/dx_2.

Experiments on homogeneous shear flows have been made at different shear rates as well as different Reynolds numbers, and both these parameters could have an effect on the non-dimensional dissipation rate. The microscale Reynolds number R_λ in these flows varies between about 110 and 440. We have first searched for possible variation with respect to R_λ by examining data in which sizeable variation in the Reynolds number occurred ($120 < R_\lambda < 360$) without comparable variation in the shear rate ($8.2 < S < 9.9$); see items with asterisks in Table 1. It appears from Fig. 2 that the Reynolds-number variation in these data is essentially negligible. We thus conclude that the Reynolds number effect is negligible at least for $R_\lambda > 100$ or so, consistent with our earlier finding [1] for grid turbulence.

7

We now analyze the scaling of the non-dimensional dissipation rate as a function of the shear parameter, S. Figure 3 shows this behavior. In spite of considerable scatter (thus the log-scale representation), it appears that there is a weak but definite trend with shear. This becomes especially obvious if we note that C for grid turbulence ($S = 0$) is unity. It is hard to be absolutely certain of this trend (because the uncertainties in measurements are large enough), but it would appear that the precise value of the non-dimensional dissipation rate $\langle\varepsilon\rangle L_{11}/\langle u_1^2\rangle^{3/2}$ depends, if only weakly, on the shear; in other words, $C = C(S)$. We know of no theoretical effort to understand this effect of finite shear. In the absence of theoretical guidance, it is difficult to say what analytical form this finite-shear effect should take. Empirically, however, a possible fit to the data is

$$C = C_0 \ exp(-\alpha S) \qquad (4)$$

where $C_0 = 1$ is appropriate to grid (or shear-free) turbulence and an approximate value of α is 0.03.

This feature of a diminishing C with respect to S appears to be further confirmed by the direct numerical simulation of a homogeneous shear flow with high shear rate [17]. Although the various quantities needed had to be inferred indirectly in this paper from a number of plots of non-dimensional quantities, it appears that $\langle\varepsilon\rangle L_{11}/\langle u_1^2\rangle^{3/2}$ for a shear rate $S = 33.6$ is approximately 0.43 (taking that same quantity for $S = 0$ to be unity). This is not at variance with Fig. 3 or Eq. (4).[4]

---

[4]Prudence demands some caution. At this stage, it is not possible to assert with full confidence that this weak trend is unrelated to the possible experimental artifact that flows with weak and strong shear differ in some systematic way in the degree to which they approximate their asymptotic state.

There are a few other experiments on homogeneous shear flows which are not included in Table 1. The reason, as already mentioned, is that the energy dissipation rate in these experiments was estimated only indirectly *via* local isotropy and Taylor's hypothesis. Fortunately, one can assess the adequacy of these latter estimates from the experiments listed in Table 1, where $\langle \varepsilon \rangle$ was obtained both directly and by local isotropy assumption. Figure 4 shows the ratio of the isotropic estimate to that measured directly. The ratio does not seem to vary significantly with Reynolds number. We believe that local isotropy holds at very high Reynolds numbers (see, for example, [18], [19]) and that this ratio would tend to unity at very large Reynolds numbers; we further tend to think that the ratio of Fig. 4 would have shown that trend if it were not masked by the scatter. However, the systematic variability of the ratio with respect to Reynolds number is probably small in the range considered here, and we might as well take it as a constant ≈ 0.75. Anyhow, this should suffice for the limited purpose for which it is employed below.

Given this ratio, we might now "correct" the energy dissipation estimates in experiments where local isotropy has been invoked. Some of these experiments are listed in Table 2,[5] and the variation of the non-dimensional energy dissipation rate is plotted against non-dimensional shear in Fig. 3. These data are consistent with the trend of the rest of the data in Fig. 3.

---

[5]Mulhearn and Luxton [14] have also obtained data in homogeneous shear flows. We have analyzed those data but found the dissipation rate to be about half as large as that in other comparable flows. We are not sure of the source of this discrepancy, and so do not comment further on these data.

3 Free shear flows

3.1 Turbulent wakes

We consider symmetric wakes of objects with large aspect ratio. For some distance behind the object, the details of its shape and other initial conditions are important to various degrees, but our premise is that such effects are small far from the body, or in the so-called far wake. The properties of nominally far wakes have been studied extensively. We restrict attention to far wakes without discussing details such as the downstream distance needed for this asymptotic state to be attained. Such considerations were discussed in [22], [23] and, in somewhat more specific detail, in [24]. We first consider, for the wake of a circular cylinder, the scaling of the average dissipation rate as a function of Reynolds number from low to moderately high Reynolds numbers. This will automatically lead to scaling considerations at the high-Reynolds-number end. Because of the inhomogeneity of the wake, properties such as the average dissipation, velocity and length scales vary across the wake. We therefore also obtain the scaling of the dissipation integrated across the wake, and compare it with semi-theoretical estimates from energy balance.

A note about notation: we denote the streamwise, normal and spanwise directions by x, y and z, respectively, and the velocities in those directions by u, v and w, respectively. The mean velocity in x-direction will be denoted by $U \equiv U(y)$. The streamwise velocity outside the wake will be designated U_o. The difference $U_o - U(y)$ is the defect velocity ω. The maximum defect velocity will be denoted by ω_o. The distance from the wake centerplane to where the defect velocity is half the maximum will be denoted by δ; that is, $\omega(\delta) = \frac{1}{2}\omega_o$. In the far wake, the mean and turbulence quantities attain

self-preservation; in particular,

$$\frac{\omega}{\omega_o} = f(\eta \ only),\tag{5}$$

where $\eta \equiv \frac{y}{\delta}$ and the entire dependence on the streamwise direction comes through the variables $\omega_o(x)$ and $\delta(x)$.

In an experiment described in [25], the energy dissipation rate was measured in the wake of a circular cylinder at various Reynolds numbers $190 < R_d \equiv U_o d/\nu < 4,500$; here d is the diameter of the cylinder. The measurements were made in the x-z plane 50 diameters behind the cylinder by measuring two velocity components U and W in that plane using Particle Image Velocimetry. Experimental details will be described elsewhere, but it suffices to note that the measurement accuracy was deemed comparable to that of hot-wire measurements. Also measured was the transverse length scale L_z defined as

$$L_z = \int\limits_0^\infty dr \frac{R_{ww}(r)}{\langle w_1^2 \rangle},\tag{6}$$

where r is the separation distance in the direction z.

Figure 5 plots $\langle \varepsilon \rangle \delta/\omega_o^3$ and $\langle \varepsilon \rangle L_z/\langle w^2 \rangle^{\frac{3}{2}}$ as a function of the cylinder Reynolds number. Both are plotted in the figure. It is clear that both these quantities decrease with Reynolds number up to about 1,000, but seem thereafter to attain a value that is independent of the Reynolds number. An extension of these measurements to higher Reynolds numbers would have been desirable. It is also true that the measurements should have been made farther downstream, but the compromise was necessary for reasons of accuracy: much further downstream, velocity fluctuations become weaker rendering their accurate measurement increasingly difficult. Even so, it is believed

11

that the trend exhibited in Fig. 4 holds true for the far wake as well. Thus, the best asymptotic estimates[6] for the centerline are:

$$\langle\varepsilon\rangle\delta/\omega_o^3 \approx 0.035 \tag{7}$$

and

$$\langle\varepsilon\rangle L_z/\langle w^2\rangle^{\frac{3}{2}} \approx 0.55. \tag{8}$$

The latter is again of order unity, as for other flows.

In another experiment at a cylinder Reynolds number R_d of 1,600 [26], we had measured 100 diameters behind the cylinder on the wake centerline the quantity $\langle\varepsilon\rangle L_x/\langle u^2\rangle^{\frac{3}{2}}$ using hot-wires. Here, L_x is the longitudinal integral scale which, except for the change of notation, is defined by Eq. (3). Our estimate is

$$\langle\varepsilon\rangle L_x/\langle u^2\rangle^{\frac{3}{2}} \approx 0.70. \tag{9}$$

Other published data (for example, [27], [16]) yield similar values, although it is difficult to be precise because of uncertainties in reading data from published small graphs: small uncertainties in velocity data could be a source of disproportionately large error in the final result. Note that the characteristic value of $\frac{\langle q^2\rangle}{\langle\varepsilon\rangle}|\frac{dU}{dy}|$ in the wake is of the order of 4.5, see appendix in Ref. [12]. For this shear parameter value, 0.7 would plot within the scatter of the data in Fig. 2.

Dissipation measurements in wakes have been made also by a number of other authors, for example [27], [16], [28], [29], [30]. The most detailed among them is Ref. [29]; the authors of Ref. [29] examine the limitations of

---

[6]For low Reynolds numbers, it appears that $\langle\varepsilon\rangle\delta/\omega_o^3 \sim R_d^{-\frac{1}{2}}$. Noting that $R_d \sim \omega_o\delta/\nu \sim \langle u^2\rangle^{1/2}L_{11}/\nu \sim R_\lambda^2$, this observation is consistent with the -1 power-law appropriate to low-Reynolds-number grid data; see Fig. 1.

local isotropy and Taylor's hypothesis and measure as many terms in Eq. (1) as possible. These measurements suggest that local isotropy underestimates the true dissipation by about the factor seen already in homogeneous shear flows. The cylinder Reynolds number R_d was 1,170 for these measurements, just barely high enough according to Fig. 5. On the basis of these data, one has

$$\frac{\langle \varepsilon \rangle \delta}{\omega_o^3} \approx 0.03 \tag{10}$$

on the wake centerline, roughly consistent with Eq. (7).[7] Since the measurements extend (more or less) all across the wake, we can obtain the scaling of the integrated dissipation as

$$\int_{-\infty}^{+\infty} d\eta \frac{\langle \varepsilon \rangle \delta}{\omega_o^3} \approx 0.1. \tag{11}$$

Other data [25], [28] yield numbers as large as 0.12.

The integrated dissipation can be estimated from the energy integral equation obtained by multiplying the Reynolds-averaged Navier-Stokes equations with the fluid velocity. By integrating the energy integral equation across the wake, one obtains

$$\frac{1}{2} \left[\frac{d\delta_e}{dx} - \int dy \frac{\langle q^2 \rangle U}{U_o^3} \right] = \frac{\nu}{U_o \Delta} + \int dy \frac{\langle \varepsilon \rangle}{U_o^3}. \tag{12}$$

Here, x is the streamwise distance from the wake-generator and all integrals are carried out between $-\infty$ and $+\infty$ in the variable y, and the so-called energy thickness δ_e is defined as

$$\delta_e = \int dy \frac{U}{U_o} \left[1 - \frac{U^2}{U_o^2} \right]. \tag{13}$$

---

[7]Townsend's measurements, when "corrected" for the underestimate due to the use of local isotropy, are also consistent with Eq. (10). Thomas [28] obtained a slightly higher value of 0.038. On the whole, a good average centerline value appears to be 0.035.

We also have the so-called mean dissipation thickness given by

$$\Delta^{-1} = \int dy \left(\frac{\partial}{\partial y} \frac{U}{U_o} \right)^2 . \tag{14}$$

At high Reynolds numbers in the far wake, it is easy to show that, to the lowest order in ω_o/U_o,

$$\int \frac{\langle \varepsilon \rangle \delta}{\omega_o^3} d\eta = \frac{1}{2} \frac{d}{dx} \delta_e = \frac{3}{4} \frac{\Delta}{\Omega} \left(I_2 - \frac{I_2'}{3} \right), \tag{15}$$

where $I_2 = \int_{-\infty}^{+\infty} (\omega/\omega_o)^2 d\eta$, $I_2' = \int_{-\infty}^{+\infty} (\langle q^2 \rangle/\omega_o^2) d\eta$, $\Omega = (\omega_o/U)(x/\theta)^{\frac{1}{2}}$, $\Delta = \delta/(x\theta)^{\frac{1}{2}}$, and θ is the momentum thickness defined as

$$\theta = \int dy \frac{U}{U_o} \left[1 - \frac{U}{U_o} \right] . \tag{16}$$

Using from Ref. [24] the numerical values of $I_2 = 1.51 \pm 0.02$, $\Omega = 1.63 \pm 0.02$ and $\Delta = 0.3 \pm 0.005$, and noting that $I_2' \approx 0.8$, we obtain

$$\int d\eta \frac{\langle \varepsilon \rangle \delta}{\omega_o^3} = 0.17. \tag{17}$$

This estimate is substantially larger than that obtained from measurement (between 0.1 and 0.12). Corrections $O(\theta/\delta)$ ignored in the estimate (17) can bring them closer, but not nearly enough. It is well-known that the asymptotic properties of the wake are attained only very far downstream, and we therefore wonder if any dissipation measurements have been made in the true far wake! Alternatively, slight streamwise pressure gradients in wind-tunnel measurements could account for this discrepancy. In spite of these pessimistic remarks, however, let us not lose sight of the degree of closeness between the two estimates.

3.2 Other unbounded shear flows

Similar analyses have been carried out for other unbounded shear flows and the results are summarized below. These estimates are not as detailed nor as solid as for homogeneous shear flows and wakes. Indeed, the question of Reynolds number variation will not be addressed at all, and it will be assumed that the values to be quoted below are representative of the high-Reynolds-number limit. Local isotropy estimates will be used in some dissipation measurements to follow, which probably means that the numbers below ought to be somewhat higher. The length scale is not obtained with the same degree of consistency as for homogeneous flows. Added to this, even elementary features such as the ratio of the root-mean-square longitudinal velocity to the mean velocity in two realizations of nominally the same flow configuration are somewhat different from one flow to another.[8]

a. Axisymmetric jets: The principal reference used is [31]. It would appear that, on the centerline of the jet far away from the nozzle,

$$\frac{\langle \varepsilon \rangle \delta}{U_o^3} \approx 0.015 \qquad (18)$$

where U_o is the velocity on the jet centerline and δ is the radial distance from the jet axis to the circle marked by half the excess mean velocity. The integrated dissipation

$$2\pi \int d\eta \frac{\langle \varepsilon \rangle \delta}{U_o^3} \, \eta \ \approx 0.11. \qquad (19)$$

---

[8]This type of inconsistency between one experiment and another is a constant source of concern. Among other implications that this may have, it results in uncertainties that cannot be quantified with any confidence. This state of affairs indicates strongly that a repetition of standard measurements (including dissipation) in high-quality canonical flows will not be a wasted effort, especially if the measurements are accompanied by improved instrumentation and data processing techniques.

On the jet axis we have,

$$\frac{\langle\varepsilon\rangle L_u}{\langle u^2\rangle^{\frac{3}{2}}} \approx 0.35, \tag{20}$$

consistent in order of magnitude with that in other flows.

For the far field, the semi-theoretical energy integral estimate for the integrated dissipation is about 0.15 instead of 0.11 from measurement. This discrepancy is comparable to that noted earlier for wakes.

Two-dimensional jets: For two-dimensional jets, we have principally used data from Refs. [32] and [33]. The two sources of data are not entirely consistent with each other. However, a typical value is

$$\frac{\langle\varepsilon\rangle\delta}{U_o^3} \approx 0.01 \tag{21}$$

where U_o is the velocity on the jet centerline and δ is defined as the distance from the jet axis to the plane marked by half the excess mean velocity. We also have

$$\frac{\langle\varepsilon\rangle L_u}{\langle u^2\rangle^{\frac{3}{2}}} \approx 0.23, \tag{22}$$

consistent again only in the order of magnitude sense with other flows. The integrated dissipation from measurement scales as

$$\int d\eta \frac{\langle\varepsilon\rangle\delta}{U_o^3} \approx 0.035. \tag{23}$$

The number from energy balance is about 0.041, with comparable discrepancies as before.

Two-dimensional mixing layers: For the mixing layers, we have used the data from [34]. For this flow,

$$\frac{\langle\varepsilon\rangle\delta}{U_o^3} \approx 0.005 \tag{24}$$

16

where U_o is the difference in velocity between the two sides of the mixing layer and δ is the distance between the planes where the mean velocities are $0.9U_o$ and $0.1\,U_o$. The integrated dissipation scales as

$$\int d\eta \frac{\langle\varepsilon\rangle\delta}{U_o^3} \approx 0.05. \tag{25}$$

On the central plane where the velocity is the mean of those on the two sides, we have

$$\frac{\langle\varepsilon\rangle L_u}{\langle u^2\rangle^{\frac{3}{2}}} \approx 0.43. \tag{26}$$

The order of magnitude is consistent with that in other shear flows.

Table 3 summarizes the scaling relations for the turbulent flows considered so far. We reiterate the tentative nature of the estimates for jets and mixing layers.

4   The turbulent boundary layer

We now turn attention to the dissipation in two-dimensional turbulent boundary layer. This flow is special for many reasons, but an important aspect is that the viscous effects are not negligible in the near-wall region (to be defined more precisely later) no matter how high the Reynolds number. It would therefore be useful to estimate the fraction of dissipation due to the mean velocity gradient. So would it be to estimate separately the energy dissipation in different parts of the boundary layer.

A convenient starting point is the energy integral equation, Eq. (12),

which can be rewritten as[9]

$$\frac{1}{2}\left(\frac{U_o}{U_*}\right)^3\frac{d\delta_e}{dx} = \frac{1}{2}\int_0^\infty dy\frac{U\langle q^2\rangle}{U_*^3} + \int_0^\infty d(yU_*/\nu)\left(\frac{\partial(U/U_*)}{\partial(yU_*/\nu)}\right)^2 + \int_0^\infty dy\frac{\langle\varepsilon\rangle}{U_*^3}. \quad (27)$$

Here, U_o is the free-stream velocity; the viscous term is non-dimensionalized by the kinematic viscosity ν and the so-called friction velocity U_* defined by $(\tau_w/\rho)^{\frac{1}{2}}$, τ_w being the shear stress at the wall. For high Reynolds numbers, the direct dissipation term due to the mean shear on the right hand side of Eq. (27) is significant only in the near-wall region (defined by $yU_*/\nu < 30$) where, to an excellent approximation, the velocity scales on U_* and the distance from the wall scales on ν/U_*; the integral is therefore essentially a universal number. An examination of several measurements near the wall[10] (e.g., [35], [36], [37], [38], [39]) yields an approximate value of the viscous term is 9.5.

For convenience, the turbulent energy dissipation in the boundary layer can be thought to consist of three mutually exclusive parts—that in the near-wall region ($yU_*/\nu < 30$, as already remarked), that in the logarithmic region ($30\nu/U_* < y < 0.2\delta$, say) and that in the outer region of the boundary layer ($y > 0.2\delta$). In the near-wall region, $\langle\varepsilon\rangle$ scales on wall variables ν and U_* and, in the outer region, on U_* and δ. The integrated dissipation can be written as

$$\int_0^\delta dy\frac{\langle\varepsilon\rangle}{U_*^3} = \int_0^{30} d\left(\frac{yU_*}{\nu}\right)\frac{\langle\varepsilon\rangle\nu}{U_*^4} + \int_{30\nu/U_*}^{0.2\delta} dy\frac{\langle\varepsilon\rangle}{U_*^3} + \int_{0.2\delta}^\delta d\left(\frac{y}{\delta}\right)\frac{\langle\varepsilon\rangle\delta}{U_*^3}. \quad (28)$$

---

[9]The first term on the right hand side is the difference between integrated production and dissipation.

[10]Since the mean velocity in the near-wall region is essentially independent of the outer region it seems reasonable to expect this number to be the same for all wall-bounded flows such as pipe and channel flows, Taylor-Couette flow and so forth. This sanguine statement cannot be made about all aspects of wall turbulence.

18

Since $\frac{\langle\varepsilon\rangle\nu}{U_*^4}$ is a unique function of $\frac{yU_*}{\nu}$ in the near-wall region and $\frac{\langle\varepsilon\rangle\delta}{U_*^3}$ is a unique function of $\frac{y}{\delta}$ in the outer region (at least for high enough Reynolds numbers), the first and the third integrals on the right hand side are pure numbers, C_i and C_o, say, independent of the Reynolds number. Estimates of C_i and C_o suffer from uncertainties already mentioned in dissipation measurements. However, the use of Klebanoff's data for the outer region and those from any of the sources mentioned above for the near-wall region yields

$$C_i \approx 3.6, C_o \approx 2.1. \tag{29}$$

Two remarks are useful. First, the present estimate for C_i is decidedly low. For example, turbulent dissipation estimate by $15\nu\langle\frac{du}{dx}\rangle^2$ yields zero at the wall whereas the true dissipation there, as given by Eq. (1), can be shown to be finite because not all fluctuating velocity gradients vanish at the wall. This estimate should therefore be treated with some reserve. In any case, it is clear that the near-wall region, which constitutes a vanishingly small part of the boundary layer (it is about one percent of the total thickness at a momentum thickness Reynolds number of 10^4), dissipates more than the outer region constituting about 80% of the boundary layer thickness.

Secondly, if one is interested in the scaling of the dissipation in regions not infested with direct viscous effects, that information is provided by the constant C_o. That is,

$$\int dy \frac{\langle\varepsilon\rangle}{U_*^3} \approx 2. \tag{30}$$

As already remarked, this is indeed independent of the Reynolds number.[11]

---

[11] For high Reynolds numbers, say $R_\theta > 6,000$, the characteristic velocity scale may be thought be about $2.5U_*$, see [41]. The rescaled integrated dissipation will then be about 0.13, not very different from that in two-dimensional wakes. This result is more

Returning to Eq. (28), one may assume in the logarithmic region of the boundary layer that $\langle \varepsilon \rangle = \frac{1}{\kappa} \frac{U_*^3}{y}$, where κ is the so-called Kàrmàn constant ≈ 0.41, and the second integral[12] can be written as $\frac{1}{\kappa} ln(\frac{1}{150} \cdot \frac{U_* \delta}{\nu})$. We thus have

$$\int_0^\delta dy \frac{\langle \varepsilon \rangle}{U_*^3} = C_i + C_o + \frac{1}{\kappa} ln \left(\frac{1}{150} \times \frac{U_* \delta}{\nu} \right). \tag{31}$$

It is clear that the integrated dissipation in the logarithmic part of the boundary layer increases without bound (albeit slowly), while those in the near-wall and outer regions remain finite and become diminishingly small fractions of that in the logarithmic region. As the Reynolds number increases, the near-wall viscous dissipation due to the mean shear becomes a vanishingly small fraction of the turbulent dissipation. However, even for reasonably high Reynolds numbers encountered in the boundary layer of Ref. [40], this fraction is about one half of the turbulent dissipation.[13] Finally, in the logarithmic region,

$$\langle \varepsilon \rangle L_u / \langle u^2 \rangle^{3/2} \approx 2, \tag{32}$$

essentially independent of the distance from the wall.

The left hand side of Eq. (27), i.e., $d\delta_e / dx$, has been evaluated for the boundary layer of Weighardt [40] in the range $450 < R_\theta < 15,500$. The difference between this term and the direct dissipation term (both normalized

---

than a coincidence given the similarities between the plane wake and the outer part of the boundary layer [42].

[12]An examination of the dissipation data from various sources shows that they do not exactly follow the relation $\langle \varepsilon \rangle = \frac{1}{\kappa} \frac{U_*^3}{y}$ in the logarithmic region. For some boundary layers, this relation holds in the lower part of the logarithmic region while, in some others, in the upper part. This estimate is good to within a factor 2. Note that, if one uses for ℓ the mixing length $\approx \kappa y$, and U^* for the velocity scale v, one would have the result $\langle \varepsilon \rangle \ell / v^3 = 1$.

[13]This ratio is related to the quantity optimized in Ref. [43].

as in Eq. (27)) is plotted in Fig. 6; we have used for the abscissae the more natural Reynolds number $U_* \delta / \nu$, where δ is the boundary layer thickness, instead of the more conventional R_θ. Even though there is some scatter, the data clearly show an increasing trend with respect to the Reynolds number. Figure 6 also plots the total dissipation (that is, sum of viscous and turbulent parts of the dissipation) evaluated according to Eqs. (31) and (29). This sum is similar in trend to the data on $(d\delta_e/dx - direct\ dissipation)$. Note that the imbalance between the data points and the total dissipation must be the second term on the right hand side of Eq. (27). The difference appears to be essentially independent of the Reynolds number and we have

$$\int \frac{\langle q^2 \rangle U}{U_*^3} dy \approx 2.4. \tag{33}$$

Figure 7 plots the same data as a fraction of the work done at the wall against friction, the latter being given by $\tau_w U_o$. The ratio is close to unity, nearly always slightly smaller, decreasing weakly with the Reynolds number. The fact that the ratio is close to unity is non-trivial (because it is not constrained to be so) and suggests that the rate of change of energy at any streamwise position is balanced essentially by the work done by the friction *locally*.

Finally, Fig. 8 plots the quantity $\frac{U_*}{U_o}[(d\delta_e/dx) - direct\ dissipation)]$. This is the fraction of the local rate of change of energy that occurs entirely due to turbulent dissipation. This ratio is a Reynolds-number-independent constant of about 0.55.

21

5 Conclusions

We have examined the question of whether energy dissipation scales in a unique way in all turbulent flows. The answer is not as satisfactory as one would desire, yet some broad conclusions can be drawn. These are summarized below.

For homogeneous shear flows, it appears that $\langle \varepsilon \rangle L_{11}/\langle u_1^2 \rangle^{\frac{3}{2}}$ is a weak function of the shear, approaching the value appropriate to grid turbulence in the limit of vanishing shear. Normalization by alternative length and velocity scales does not alter this conclusion in a significant way. If this conclusion is correct, we can imagine a situation in which various exponents in turbulence are also weakly dependent on the shear. Strictly speaking, then, the effect of mean shear might never disappear but manifest itself weakly at all Reynolds numbers.

For inhomogeneous flows, the basic question is one of how much energy is dissipated across the entire flow width. We have tried to answer this question for a few canonical flows. The numerical values for the integrated dissipation are different from one flow to another if one uses the *natural* velocity and length scales (for the wake, for example, these could be the maximum defect velocity and the half-defect thickness). Even if one uses the integral length scale (measured in nominally the same way) and the root-mean-square velocity in the streamwise direction, the numerical values are not the same in all flows, although they are all of order unity. This is true even in the case of the boundary layer when the outer region is considered. This conclusion, although weak and not different from prevailing wisdom, is already interesting. As is well known, in Kolmogorov's phenomenology [4]

without intermittency effects, one has the relation

$$\langle \Delta u_r^2 \rangle = C_k \langle \varepsilon \rangle^{2/3} r^{2/3} \tag{34}$$

where the velocity increment $\Delta u_r \equiv u(x + r) - u(x)$, u is the fluctuating velocity in the direction x, r is the separation distance along x, and C_k is a universal constant. If we assume that the scaling formula given by Eq. (34) extends all the way up to the longitudinal integral scale L_u, we would have (since $\langle \Delta u_r^2 \rangle \to 2\langle u^2 \rangle$ for large r, for reasons of statistical independence and statistical homogeneity at the scale L_u)

$$\frac{\langle \varepsilon \rangle L_u}{\langle u^2 \rangle^{3/2}} = \left(\frac{2}{C_k} \right)^{3/2} . \tag{35}$$

It is known empirically that C_k lies between 1.8 and 2.2 (see [2]), which gives

$$\frac{\langle \varepsilon \rangle L_u}{\langle u^2 \rangle^{3/2}} = 1 \pm 0.15. \tag{36}$$

This variation is not large enough to account for the variability of C observed in Table 2. In practice, however, there is no reason to expect the scaling to extend exactly to L_u; more likely, it holds up to an L_{eff} which is a fraction (or multiple) of L_u. Further, if $\langle \Delta u_r^2 \rangle \big|_{r=L_{eff}} = \beta \langle u^2 \rangle$, where β is of order 2 (but not exactly so), we would have, instead of Eq. (35),

$$\frac{\langle \varepsilon \rangle L_u}{\langle u^2 \rangle^{3/2}} = \alpha \left(\frac{2}{C_k} \right)^{3/2} , \tag{37}$$

where $\alpha = (L_u/L_{eff})(2/\beta)^{3/2}$. If $L_{eff} < L_u$, it is conceivable that $\beta < 2$ and $\alpha > 1$. On the other hand, if $L_{eff} > L_u$, one might have $\alpha < 1$, as observed. In this perspective, α would be a function of the flow.

Finally, we have dealt with a few other specific questions. Among them are the low-Reynolds-number behavior of this scaling for wakes, the application of energy balance for obtaining the integrated energy dissipation, the

23

contribution of viscous dissipation to the total energy dissipation in turbulent boundary layer, and so forth. We have particularly pointed out that, even in the boundary layer, the viscous contribution near the wall vanishes as the Reynolds number increases, but this rate of decrease is quite slow: Even at an R_θ of about 15,000, this fraction is still about a third of the total energy dissipation. The contributions to the turbulent energy dissipation from the near-wall region and the outer region are estimated, and the latter is shown to be comparable to that in plane wakes. The logarithmic region eventually dominates the boundary layer dissipation. We also find that the rate of change of energy at any streamwise position is balanced essentially by the work done *locally* by the friction at the wall.

References

[1] K.R. Sreenivasan, Phys. Fluids 27, 1048 (1984)

[2] A.S. Monin and A.M. Yaglom, *Statistical Fluid Mechanics* (MIT Press, Cambridge, 1971), vol. II

[3] G.I. Taylor, Proc. Roy. Soc. Lond. A 151, 421 (1935)

[4] A.N. Kolmogorov, Dokl. Akad. Nauk. SSSR 30, 301 (1941)

[5] C. Doering and P. Constantin, Phys Rev E. 49, 4087 (1994)

[6] L.N. Howard, Annu. Rev. Fluid Mech. 4, 473 (1972)

[7] G.K. Batchelor, *The Theory of Homogeneous Turbulence* (Cambridge University Press, England, 1953)

[8] P.G. Saffman, in *Topics in Nonlinear Physics*, edited by N. Zabusky (Springer, Berlin, 1968)

[9] F.H. Champagne, V.G. Harris, and S. Corrsin, J. Fluid Mech. 41, 81 (1970)

[10] V.G. Harris, J.A. Graham, and S. Corrsin, J. Fluid Mech. 81, 657 (1977)

[11] S. Tavoularis and S. Corrsin, J. Fluid Mech. 104, 311 (1981)

[12] K.R. Sreenivasan, J. Fluid Mech. 154, 187 (1985)

[13] S. Tavoularis and U. Karnik, J. Fluid Mech. 204, 457 (1989)

[14] P.J. Mulhearn and R.E. Luxton, J. Fluid Mech. 68, 577 (1975)

[15] G. Comte-Bellot and S. Corrsin, J. Fluid Mech. 48, 273 (1971)

[16] A.A. Townsend *The Structure of Turbulent Shear Flows* (Cambridge University Press, Cambridge, England, 1978, second edition)

[17] M.J. Lee, J. Kim and P. Moin, J. Fluid Mech. 216, 561 (1990)

[18] K.R. Sreenivasan, Proc. Roy. Soc. Lond. 434, 165 (1991)

[19] S. G. Saddoughi and S. Veeravalli, J. Fluid Mech. 268, 333(1994)

[20] W.G. Rose, J. Fluid Mech. 25, 97 (1966); 44, 767 (1970)

[21] J.J. Rohr, E.C. Itsweire, K.N. Helland, and C.W. Van Atta, J. Fluid Mech. 187, 1 (1988)

[22] R. Narasimha and A. Prabhu, J. Fluid Mech. 54, 1 (1972)

[23] A. Prabhu and R. Narasimha, J. Fluid Mech. 54, 19 (1972)

[24] K.R. Sreenivasan and R. Narasimha, Trans. ASME, J. Fluids Engg., 104, 167 (1982)

[25] A.K. Suri, A. Juneja, and K.R. Sreenivasan, Bull. Amer. Phys. Soc. (abstract only),vol. 36 (1991)

[26] P. Constantin, I. Procaccia and K.R. Sreenivasan, Phys. Rev. Lett. 67, 1739 (1991)

[27] A.A. Townsend *The Structure of Turbulent Shear Flows* (Cambridge University Press, Cambridge, England, 1956)

[28] R.M. Thomas, J. Fluid Mech. 57, 545 (1973)

[29] L.W.B. Browne, R.A. Antonia and D.A. Shaw, J. Fluid Mech. 179, 307 (1987)

[30] C. Meneveau and K.R. Sreenivasan, J. Fluid Mech. 224, 429 (1991)

[31] I. Wygnanski and H. Fiedler, J. Fluid Mech. 38, 577 (1969)

[32] E. Gutmark and I. Wygnanski, J. Fluid Mech. 73, 465 (1976)

[33] K.W. Everitt and A.G. Robins, J. Fluid Mech. 88, 563 (1978)

[34] I. Wygnanski and H. Fiedler, J. Fluid Mech. 41, 327 (1971)

[35] J. Laufer, *Investigation of turbulent flow in a two-dimensional channel*, NACA Rep. 1053, 1951

[36] J. Laufer, *The structure of turbulence in fully developed pipe flow*, NACA Rep. 1174, 1954

[37] P.S. Klebanoff, *Characteristics of turbulence in a boundary layer with zero pressure gradient*, NACA Rep. 1247, 1955

[38] G. Comte-Bellot, *Turbulent flow between two parallel walls*, ARC Rep. 31609, FM 4102, 1969 (A 1963 Ph.D. thesis in French translated into English by P. Bradshaw.)

[39] H. Ueda and J.O. Hinze, J. Fluid Mech. 67, 125 (1975)

[40] For tabulation of the boundary layer data, see D.E. Coles and E.A. Hirst, *Proceedings of computation of turbulent boundary layers: 1968 AFOSR-IFP-Stanford Conference, Vol. II*, 1968. pp. 100-123.

[41] D.E. Coles, *The turbulent boundary layer in compressible fluid*, RAND Rep. R-403-PR, Rand Corporation, Santa Monica, CA, 1962

[42] D.E. Coles, J. Fluid Mech. 1, 191 (1956)

[43] L.M. Smith and W.V.R. Malkus, J. Fluid Mech. 208, 479 (1989)

source	R_λ	S	$\dfrac{\langle\varepsilon\rangle L_{11}}{\langle u_1^2\rangle^{3/2}}$	$\dfrac{\langle\varepsilon\rangle L_{11}}{\langle q^2/3\rangle^{3/2}}$
Champagne et al. [9]	150	6.0	1.20	1.90
Harris et al. [10]	300	11.7	0.67	1.24
Tavoularis and Corrsin [11]	245	12.5	0.55	1.15
Sreenivasan [12]	250	9.0*	0.65	1.10
Tavoularis and Karnik [13]	440	6.4	0.75	1.47
"	360	9.6*	0.50	0.90
"	270	9.0*	0.65	1.16
"	120	9.9*	0.66	1.18
"	140	9.2*	0.62	1.09
"	160	8.2*	0.70	1.25
"	–	5.9	0.73	1.54
"	–	6.2	0.70	1.56
"	–	8.0	0.69	1.51
"	–	8.3*	0.70	1.64
"	–	9.3*	0.45	0.94
"	–	8.5*	0.45	0.95

Table 1: Principal results from experiments in which all the needed quantities were measured. Asterisks are explained in the text.

source	R_λ	S	$\dfrac{\langle\varepsilon\rangle L_{11}}{\langle u_1^2\rangle^{3/2}}$	$\dfrac{\langle\varepsilon\rangle L_{11}}{\langle q^2/3\rangle^{3/2}}$
Rose [20]	120	6.5	1.05	1.67
Rohr et al. [21]	110	11.0	0.53	1.10
"	130	12.0	0.55	1.15

Table 2: Typical data deduced by "correcting" the measured energy dissipation rate, as described in the text.

flow	v	ℓ	$C = \frac{\langle\varepsilon\rangle\ell}{v^3}$	integrated dissipation
grid turbulence	$\langle u_1^2\rangle^{\frac{1}{2}}$	L_{11}	1.0	–
homogeneous shear flows	$\langle u_1^2\rangle^{\frac{1}{2}}$	L_{11}	$C = C(S)$	–
two-dimensional wake	$\langle u_1^2\rangle^{\frac{1}{2}}$	L_{11}	0.7	
two-dimensional wake	ω_o	δ	0.035	0.10-0.12
two-dimensional jet	$\langle u_1^2\rangle^{\frac{1}{2}}$	L_{11}	0.35	
two-dimensional jet	U_o	δ	0.015	0.11
axisymmetric jet	$\langle u_1^2\rangle^{\frac{1}{2}}$	L_{11}	0.23	
axisymmetric jet	U_o	δ	0.01	0.035
2-D mixing layer	$\langle u_1^2\rangle^{\frac{1}{2}}$	L_{11}	0.43	
2-D mixing layer	U_o	δ	0.005	0.05

Table 3: Summary of dissipation results for unbounded shear flows. For inhomogeneous flows, the values quoted are for the centerline. The length and velocity scales have been defined in the text. Note that $C(S) = exp(-0.03S)$.
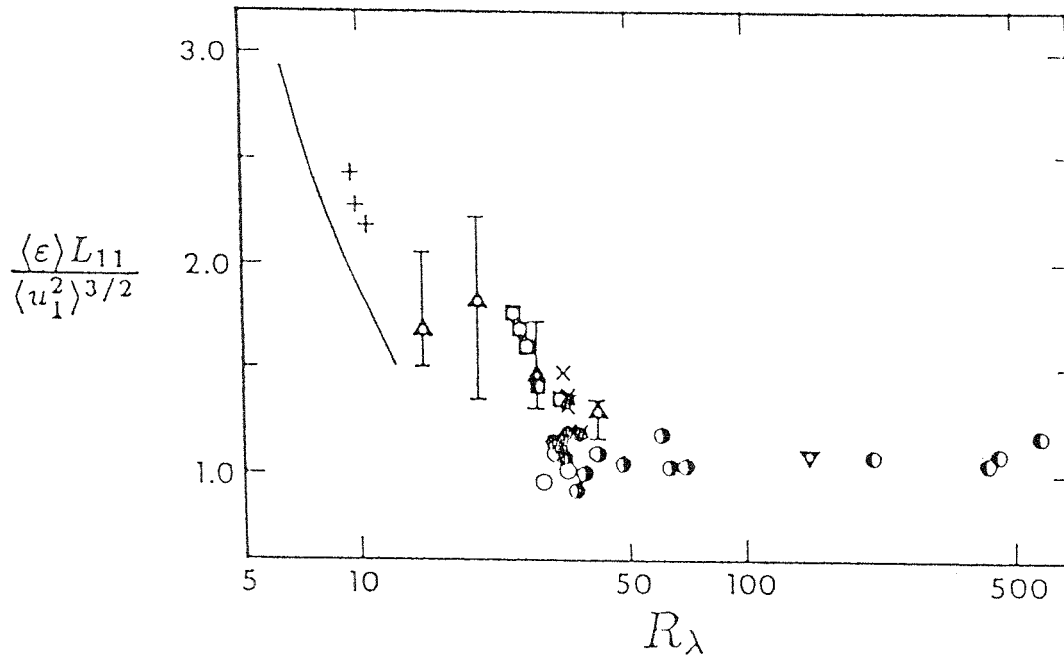
Figure 1: The average energy dissipation rate scaled on the energy-containing scales of turbulence, plotted against the microscale Reynolds number $R_\lambda \equiv \langle u_1^2 \rangle^{1/2} L_{11}/\nu$. The data are for biplane square-mesh grids. The line to the left corresponds to the weak turbulence in the final period of decay in grid turbulence, and is valid in the limit of vanishing Reynolds number. The figure is reproduced from Ref. [1], where the data sources and other details can be found.
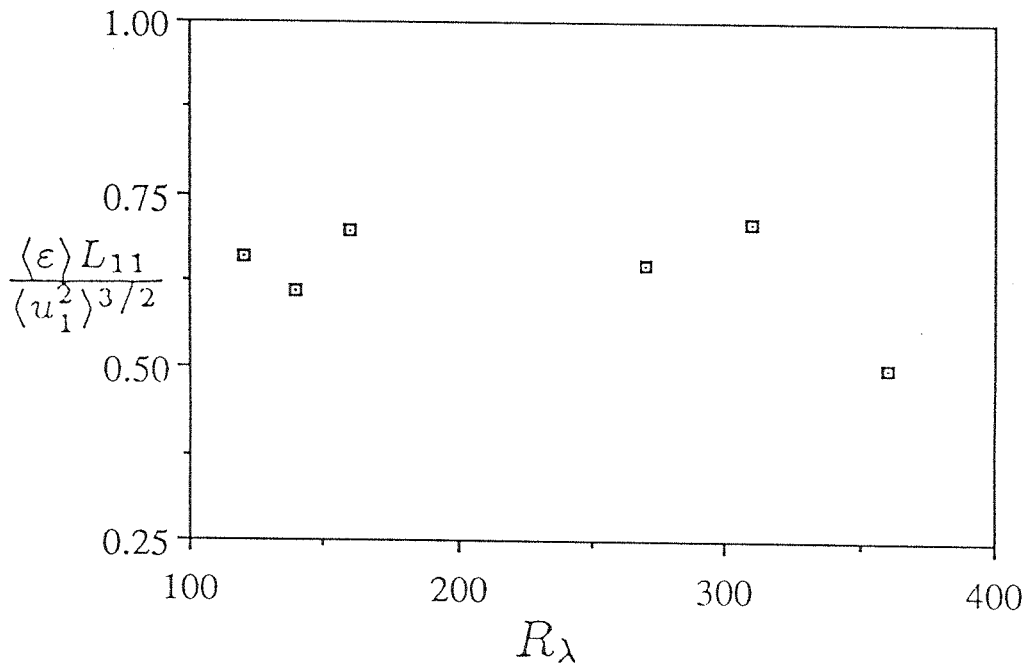
Figure 2: The average energy dissipation rate normalized on L_{11} and $\langle u_1^2 \rangle^{1/2}$ as a function of R_λ for flows with the shear parameter S in a narrow range, as described in the text. Within this range of R_λ, no clear trend with Reynolds number is apparent.
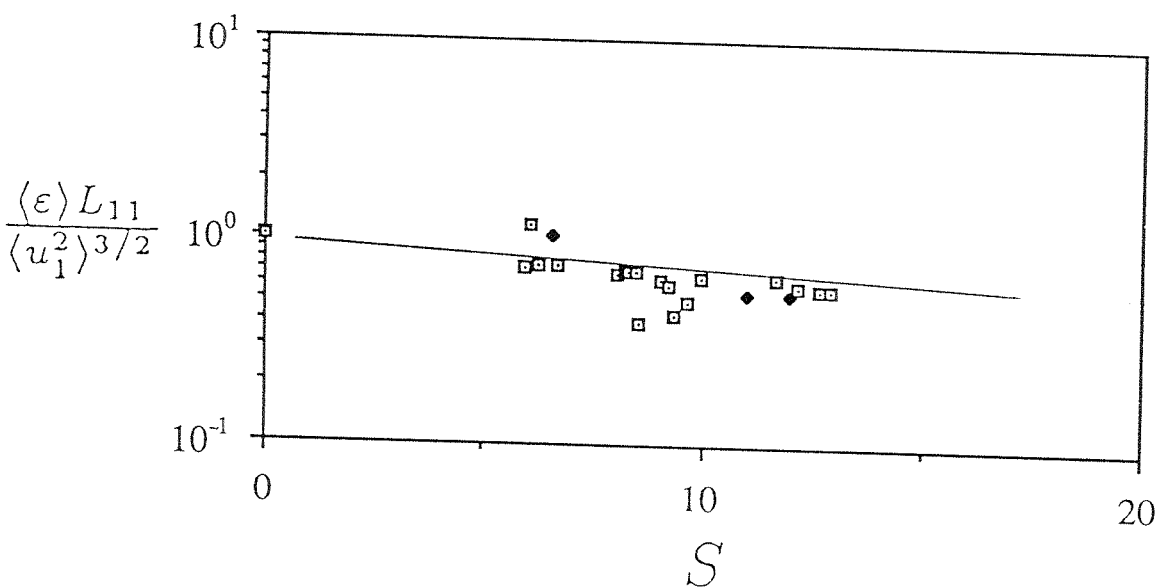
Figure 3: The average energy dissipation rate normalized on L_{11} and $\langle u_1^2 \rangle^{1/2}$ as a function of S. The squares correspond to the experiments listed in Table 1, and the diamonds to those listed in Table 2. The line corresponds to $exp(-0.03S)$.
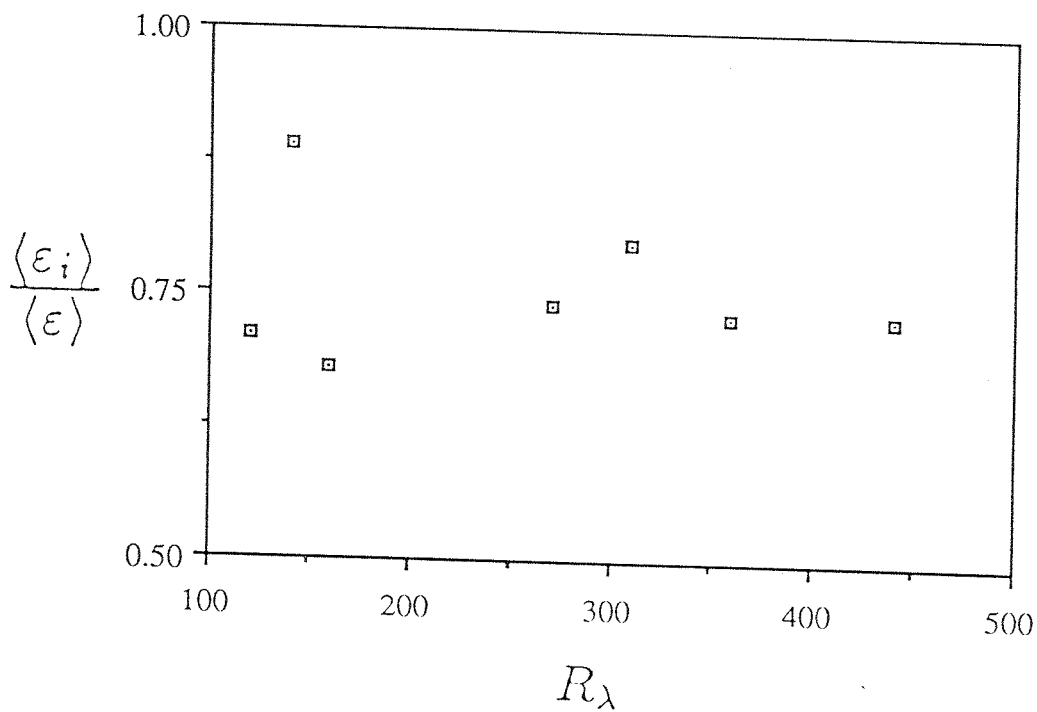
Figure 4: The ratio of the isotropic dissipation rate to that measured *via* energy balance in homogeneous shear flows. To a first approximation, this ratio can be treated as a constant within the Reynolds number range considered here.
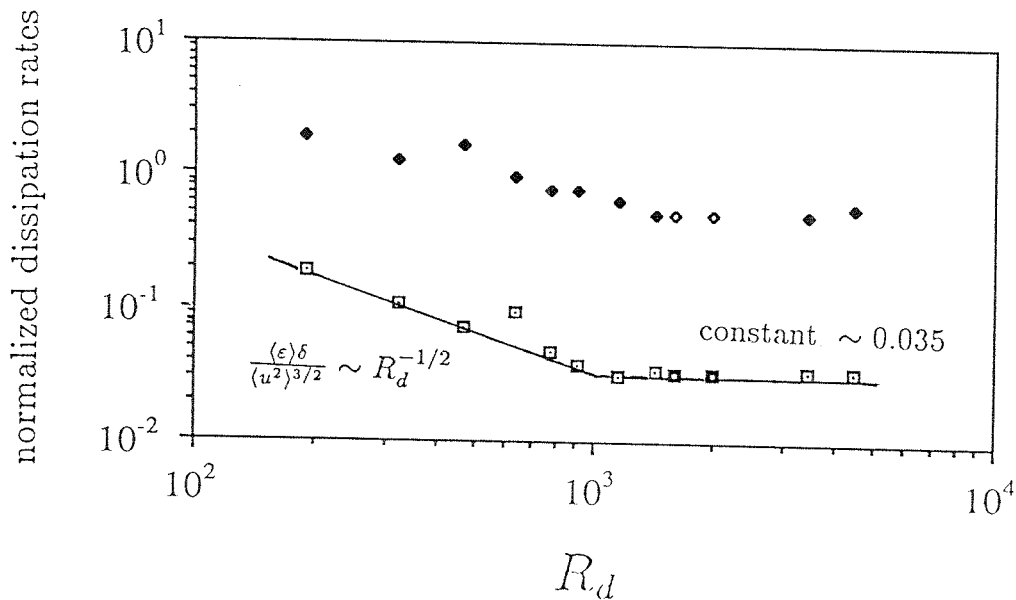
Figure 5: The quantities $\frac{\langle\varepsilon\rangle L_u}{\langle u^2\rangle^{3/2}}$, diamonds, and $\frac{\langle\varepsilon\rangle\delta}{\langle u^2\rangle^{3/2}}$, squares, plotted against the cylinder Reynolds number, R_d. For the latter, the data at low Reynolds numbers seem to show a $R_d^{-1/2}$ dependence and settle down to a constant of about 0.035 for $R_d > 1000$. The power-law behavior (if one exists) for the former quantity has a substantially smaller exponent (as should be expected from the relation between the two varieties of scales).
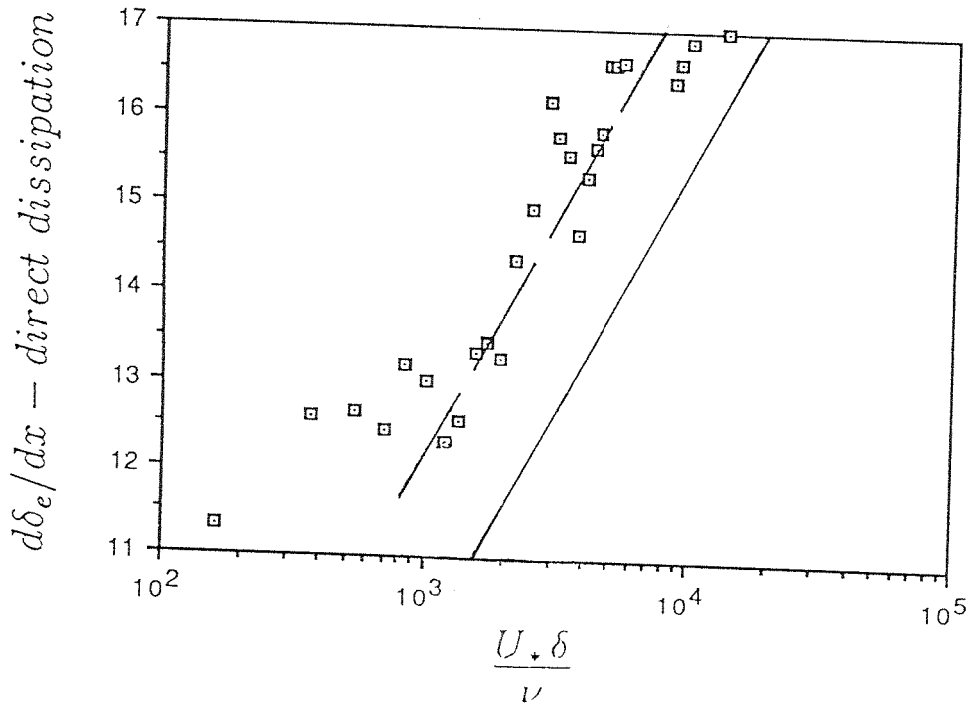
Figure 6: The quantity $(d\delta_e/dx - \textit{direct dissipation})$ for the Weighardt boundary layer, normalized as in Eq. (27). The line indicates the turbulent energy dissipation rate given by Eqs. (31) and (29). The difference between the two corresponds to $\int dy \frac{\langle q^2 \rangle U_o}{U_*^3}$.
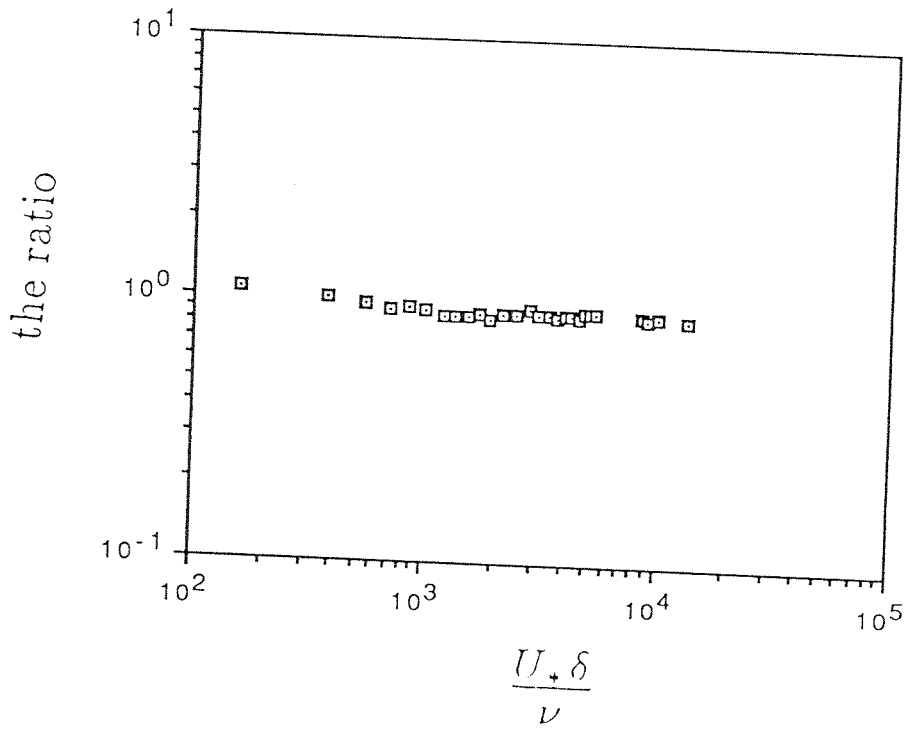
Figure 7: The ratio of $(d\delta_e/dx - direct\ dissipation)$ to the work done at the wall by friction.
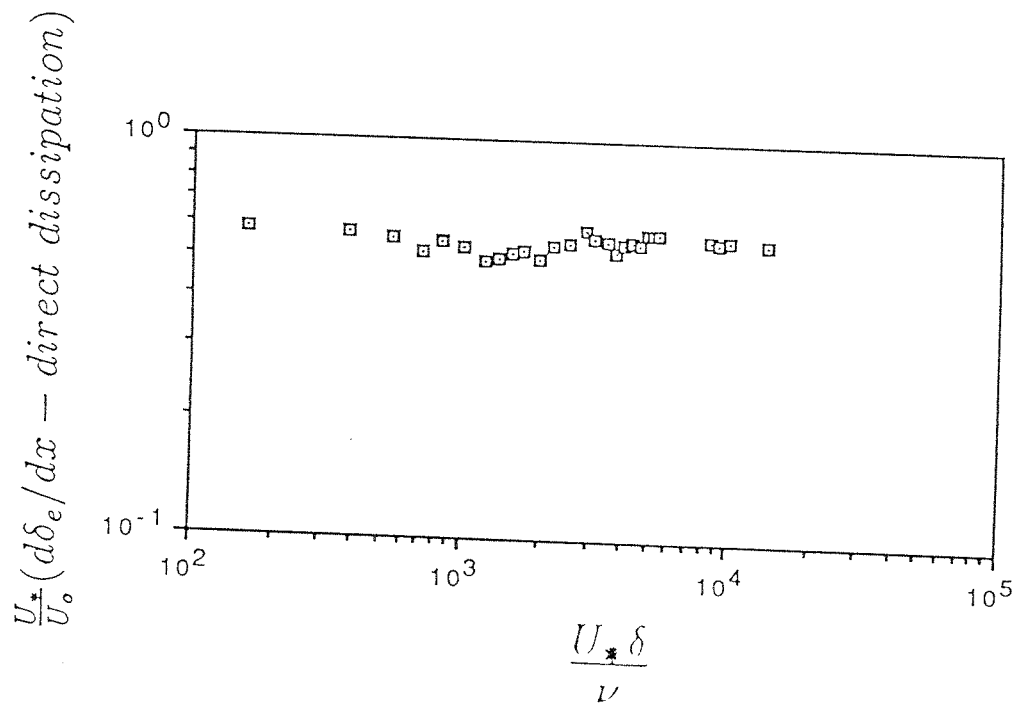
Figure 8: The quantity $\frac{U_*}{U_o}(d\delta_e/dx - direct\ dissipation)$ as a function of Reynolds number for the Weighardt boundary layer.